Miniemulsification in High-Pressure Homogenizers

Mihaela Manea, Abraham Chemtob, María Paulis, José C. de la Cal, María J. Barandiaran, and José M. Asua
Institute for Polymer Materials (POLYMAT) and Grupo de Ingeniería Química, Dept. de Química Aplicada,
Facultad de Ciencias Químicas, The University of the Basque Country, Apdo 1072, 20080 Donostia-San Sebastián, Spain

DOI 10.1002/aic.11367
Published online November 13, 2007 in Wiley InterScience (www.interscience.wiley.com).

The mechanisms involved in the formation of high solids content composite polymer–monomer waterborne miniemulsions in a high-pressure homogenizer were investigated combining experimental results and a mathematical model for the process. It was found that the final droplet size was the result of two consecutive processes: droplet break-up and coagulation. The final droplet size was determined by the mechanism giving the largest droplet size © 2007 American Institute of Chemical Engineers *AIChE J,* 54: 289–297, 2008
Keywords: miniemulsion, homogenizer, miniemulsification model, polymer-monomer

Introduction

Liquid–liquid dispersion and the closely related gas–liquid dispersion have been very active research fields because of the practical importance of these systems in processes such as liquid–liquid extraction; absorption; fermentation reactors; dairy, pharmaceutical, and cosmetic industries; polymer blends; and suspension polymerization.[1–4] Most of these works involved droplets (or bubbles) in the supermicron range, and when the submicron range was explored, rarely the size of the dispersed phase was below 250 nm. In addition, the volume fraction of the dispersed phase was in most cases below 20% and, in general, the viscosity of the dispersed phase was low. Miniemulsion polymerization is a promising route to produce composite films by casting the resulting latex.[5–8] It is expected that new and improved properties will be achieved by forming phases at nanoscale level. This requires obtaining composite miniemulsions with droplet sizes below 100 nm and relatively high viscosities of the dispersed phase (e.g., for the case of polymer–polymer nanocomposites). In addition, high solids content (about 50 wt %) is required for most practical applications. Droplet formation under these conditions has not been thoroughly investigated.

Correspondence concerning this article should be addressed to J. M. Asua at jm.asua@ehu.es.

In this work, the formation of high solid content composite polymer–monomer waterborne miniemulsions in a high-pressure homogenizer was investigated. High-pressure homogenizers seem to be the best choice for scaling up of the miniemulsification process,[6] as they are already used in the high tonnage dairy industry. The mechanisms involved in the formation of the droplets were elucidated by combining experimental results and a mathematical model for the process.

Experimental

Materials

Technical grade monomers, methyl methacrylate (MMA) and butyl acrylate (BA) supplied by Quimidroga, and acrylic acid (AA, Aldrich) were used as received. A long chain acrylate (*n*-octadecyl acrylate, SA) was used as a reactive costabilizer; Dowfax 2A1 (alkyldiphenyloxide disulfonate, Dow Chemicals) was used as a surfactant. An air drying long-oil alkyd resin (Setal 293 XX-99, Nuplex) was used. Setal 293 XX-99 is a high-solid alkyd with about 1.6% of xylene, with an acid value of 8–11 mg KOH/g and a viscosity (23°C, 100 s^{-1}) of 0.7–1.4 Pa s.

Miniemulsification

Fifty weight percent solids miniemulsions were prepared by dispersing an organic phase in an aqueous phase. The organic phase was prepared by dissolving a given amount of

alkyd resin (5–50 wt % based on the total organic phase) in a mixture of acrylic monomers (MMA/BA/AA: 49.5/49.5/1 wt/wt). A 4 wt % (based on the acrylic monomers) of a reactive costabilizer (stearyl acrylate) was also added to the solution. The aqueous phase was prepared by dissolving Dowfax 2A1 (2, 4, and 6 wt % based on organic phase) in water.

The organic and the aqueous phases were mixed under mechanical agitation, and then the droplet size was reduced by sonicating the emulsion with a Branson Sonifier (405 W and duty cycle of 90%). This was done because, as it is shown in Figure 1, the number of cycles needed to achieve the smallest droplet size in the Manton Gaulin homogenizer decreased as the droplet size of the feed decreased.[9]

The fine emulsion produced by sonication was homogenized in a two-valve Manton-Gaulin (LAB 60.10) in a loop arrangement. In this arrangement, a cycle is defined by the time needed to pass the volume of the storage tank through the homogenizer. The pressure of the first valve was varied from 6.9×10^6 Pa to 41.4×10^6 Pa. The pressure of the second valve was maintained at 10% of the pressure of the first valve.

Characterization

Droplet *z*-average diameters were determined by dynamic light scattering using a Coulter N4-Plus. Surface tension was measured by means of a tensiometer KSV Sigma 70, using the du Noüy ring method. The viscosity of the miniemulsions was measured using a Viscosimeter UK, model ELV-8. The elongational viscosity of the organic phases was measured in an extensional rheometer HAAKE CaBER 1.

Results

Preliminary miniemulsification experiments showed that the viscosity of the miniemulsions strongly increased with the alkyd resin content. These miniemulsions were difficult to handle and to feed to the homogenizer. Surprisingly, the size of the droplets of some of these high viscosity miniemulsions was relatively large (>200 nm). For this size range, no high viscosity is expected for 50 wt % dispersions, unless strong particle–particle interaction occurs.[10] In those miniemulsions, the ionic strength was low because no ions other than those of the Dowfax 2A1 were present. Therefore, the electrical double layer surrounding the particles was very thick and the electrostatic interaction was strong.

The problem was overcome by adding some amount of $NaHCO_3$ to the aqueous phase (0.024 M for the miniemulsions prepared with 2 and 4 wt % of Dowfax 2A1 and 0.039 M for 6 wt % of Dowfax 2A1).

Figures 2–4 present the effect of the pressure used in the homogenizer on the droplet size for different contents of

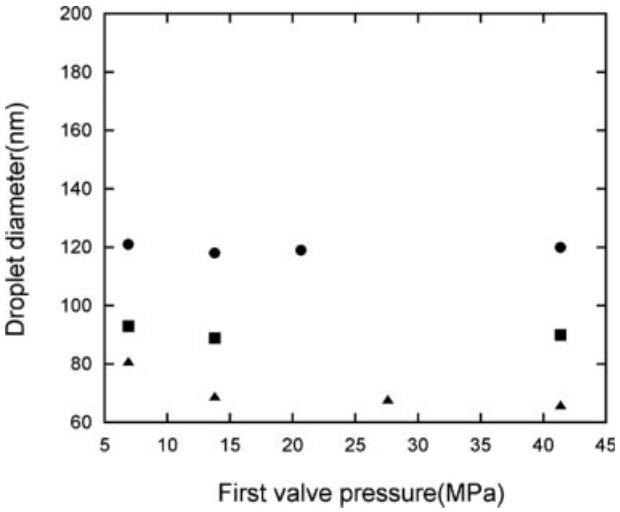

Figure 2. Effect of the pressure used in the homogenizer on the droplet size for 15 wt % of resin and different emulsifier concentrations: ● 2 wt %; ■ 4 wt %; ▲ 6 wt %.

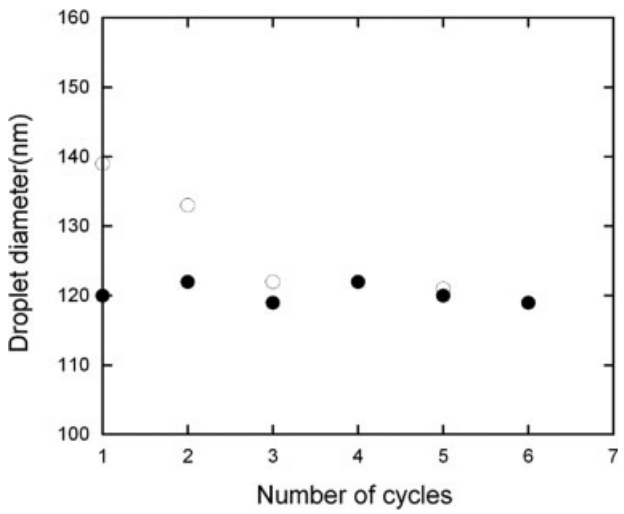

Figure 1. Effect of the presonication on the performance of the high-pressure homogenizer.

● presonication before passing from the high-pressure homogenizer; ○ without presonication.

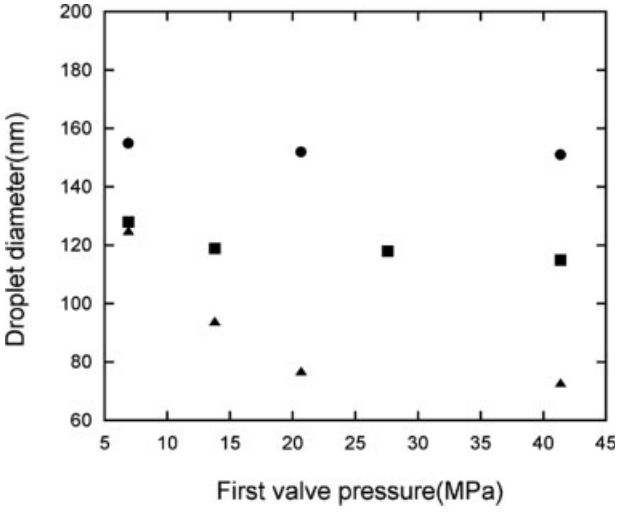

Figure 3. Effect of the pressure used in the homogenizer on the droplet size for 30 wt % of resin and different emulsifier concentrations: ● 2 wt %; ■ 4 wt %; ▲ 6 wt %.

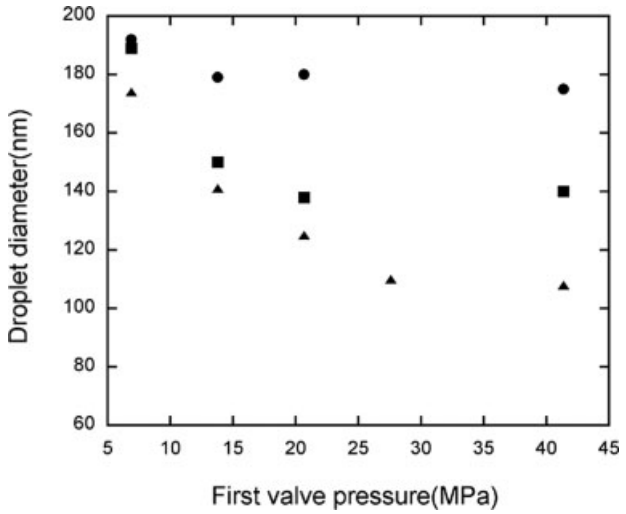

Figure 4. Effect of the pressure used in the homogenizer on the droplet size for 50 wt % of resin and different emulsifier concentrations: ● 2 wt %; ■ 4 wt %; ▲ 6 wt %.

resin (15, 30, and 50 wt %) and emulsifier concentrations (2, 4, and 6 wt %). In addition, Table 1 presents the effect of the emulsifier concentration on droplet size for miniemulsions prepared at 41.4×10^6 Pa with 5 wt % of resin. The surface tensions of these miniemulsions are presented in Table 2. Table 3 compares the relative surface areas of the miniemulsions at 41.4×10^6 Pa. Figure 5 presents the effect of the emulsifier (Dowfax 2A1) concentration on the surface tension of an aqueous solution of $NaHCO_3$ (0.024 M). Comparison of this plot with Table 2 and the concentration of emulsifier used shows that most of the emulsifier was located on the droplets.

The following information can be extracted from Figures 2 to 5 and Tables 1 and 3:

i. Droplet size decreased with the concentration of emulsifier.

ii. At low emulsifier concentrations, droplet size was almost not affected by homogenization pressure.

iii. At high emulsifier concentrations, the droplet size initially decreased with pressure and remained constant at higher values of the homogenization pressure.

iv. For a given resin content, the ratio (surface area/emulsifier concentration) decreased with the emulsifier concentration.

v. For a given homogenization pressure and emulsifier concentration, droplet size increased with the resin content.

vi. The total surface area stabilized by a given emulsifier concentration decreased with the resin content.

Results (i)–(iv) suggest that the droplet size was the result of two consecutive processes: droplet break-up (presumably occurring in the homogenizer valve) and coagulation of newly formed droplets insufficiently covered by the emulsifier (likely occurring after the homogenizer valve). At low pressures and high emulsifier concentrations, the amount of emulsifier was enough to stabilize the droplets formed in the homogenizer. Therefore, the size of the droplets decreased with the pressure in the valve. As pressure increased, the size of the droplets formed in the valve decreased and, at one point, the concentration of emulsifier was not enough to efficiently cover the surface and coagulation occurred until the surface area of the droplets decreased to a level that could be stabilized by the emulsifier available. For higher pressures, the size of the droplets was determined by the concentration of emulsifier. At low emulsifier concentrations, the size of the droplets was controlled by the concentration of emulsifier in the whole range of pressures, because the homogenizer was able to break up the droplets to sizes that gave a surface area that could not be stabilized by the emulsifier. Therefore, the droplet size was determined by the mechanism (droplet break-up vs. stabilization) giving the largest droplet size.

In this context, it is worth pointing out that stability is not a thermodynamic concept but a kinetic one. This means that stability depends on both, the coverage of the surface area and the concentration of droplets. Actually, Result (iv) illustrates this concept because the surface coverage of the droplets increased with the amount of emulsifier under conditions in which the droplet size was determined by coagulation (pressure, 41.4×10^6 Pa; Table 3). The reason was likely that the number of droplets formed in the homogenizer valve increased with emulsifier concentration, and hence their collision rate also increased, requiring a higher coverage to be stable.

At first sight (e.g., comparing the droplet sizes obtained at 13.8 MPa and 6 wt % of emulsifier with 30 and 50 wt % of resin), Result (v) suggests that the effect of the resin was to increase the viscosity of the organic phase, making it more difficult for droplet break-up. However, Figures 2–4 show

Table 1. Effect of Emulsifier Concentration on Droplet Size for Miniemulsions Prepared at 41.4 MPa with 5 wt % of Resin

Emulsifier wt %*	d (nm)
2	95
4	72
6	66

*wt % with respect to organic phase.

Table 2. Surface Tensions (mN/m) of the Miniemulsions Prepared with Different Resin Contents at Different Pressures

	5% Resin	15% Resin	30% Resin	50% Resin
First valve pressure 41.4 MPa				
2% emulsifier	34.3	33.7	34.7	38.6
4% emulsifier	33.1	34.2	35.8	37.5
6% emulsifier	35.5	35.4	35.2	35.5
First valve pressure 6.9 MPa				
2% emulsifier	–	34.5	34.1	35.9
4% emulsifier	–	32.8	33.9	34.7
6% emulsifer	–	33.3	34.1	33.9

Table 3. Relative Surface Areas of the Miniemulsions Prepared with Different Resin Contents at ΔP = 41.4 MPa (Referred to 5 wt % Resin and 2 wt % Emulsifier)

	5% Resin	15% Resin	30% Resin	50% Resin
2% emulsifier	1	0.79	0.62	0.54
4% emulsifier	1.32	1.04	0.8	0.68
6% emulsifier	1.44	1.44	1.30	0.88

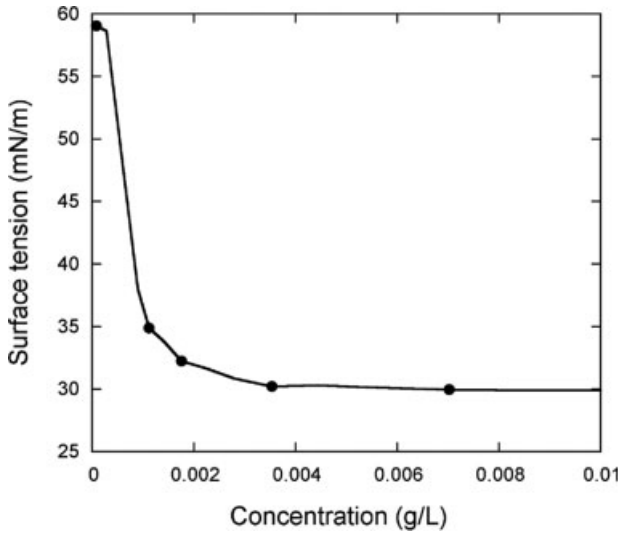

Figure 5. Effect of the emulsifier concentration on the surface tension of an aqueous solution of $NaHCO_3$ (0.024 M).

that droplet size increased with resin content even under conditions in which the size was controlled by droplet coagulation [Result (vi)]. The alkyd resin used in those experiments was hydrophobic, and therefore it may be argued that as the emulsifier adsorbed stronger on hydrophobic surfaces it could not move fast enough to the newly formed surfaces. The stronger adsorption is related to a lower value of the area covered by a molecule of emulsifier (parking area), and it is well known that the parking area decreases with the hydrophobicity of the organic phase.[11] This is confirmed by the results presented in Table 2, which showed that, for a given concentration of emulsifier, the surface tension of the miniemulsion increased with alkyd resin contents even though the total surface area of the droplets decreased. However, the droplet sizes reported were those corresponding to a high number of cycles in the homogenizer, i.e., when no further reduction of the droplet size was observed. Under these circumstances, the relative increase of the droplets' surface area caused by droplets break-up as they passed through the valve should be limited because the droplets were already small. Therefore, it is unlikely that under the conditions in which the miniemulsion were prepared, the stronger adsorption of the emulsifier on droplets containing increasing amounts of alkyd resin was the reason for the larger droplet sizes observed.

Preferential burying of the emulsifier within the droplets containing higher concentrations of alkyd resin was considered unlikely, because although this effect is known for nonionic emulsifiers, it has not been reported for anionic emulsifiers.[12,13]

Another possible explanation for the effect of the resin content on the droplet size under conditions in which the size was controlled by coalescence was that the coagulation rate of the droplets increased with the resin content. The system was electrostatically stabilized and the surface charge concentration increased with the resin content (because the total surface area decreased). Therefore, the effective Hamaker constant should increase with the resin contents. A mathematical model for the homogenization process was developed to assess this alternative.

Mathematical Model

Description of the process

The process through which the miniemulsion droplets are formed is illustrated in Figure 6. The coarse emulsion is pumped through the narrow gap of the valve where droplets break-up. CFD calculations show that in this valve there are different flow regimes.[14] At the entrance of the gap the flow lines converge, producing both shear and extensional deformation of the fluid, but extensional effects dominate. The flow through the gap is basically shear flow with a parabolic profile (Poiseuille flow). The decrease in the velocity of the fluid is very pronounced once it leaves the valve. Therefore, the fluid does not strongly impact the valve wall, but in this area turbulent flow occurs. Maximum turbulence intensity occurs at the exit of the valve. In a single valve equipment, pressure at the exit of the gap is low, and hence cavitation is possible. This is not the case for a two-valve homogenizer. Therefore, the coarse emulsion flowing through the valve will suffer elongational flow; Poiseuille flow and turbulence. In the elongational flow, the velocity gradient is in the direction of the flow. It is known that elongational flow may break up droplets of high viscosity ratios η_d/η_c (d: dispersed phase; c: continuous phase).[15] In addition, in elongational flow the shearing force acting on the drop becomes larger as the drop becomes more deformed. According to Floury et al.,[16] the time that the droplets spend at the entrance of the gap is too short to break the droplet, even though this deformation is important to facilitate the break-up later. It is

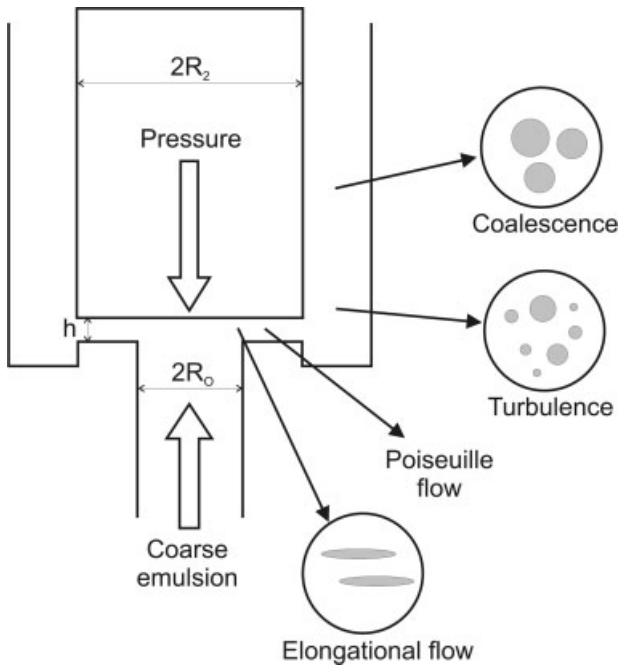

Figure 6. Miniemulsion formation in a high-pressure homogenizer.

interesting to point out that the maximum extensional strain rate occurs just before the entrance of the gap[17] and it decreases rapidly after entering the gap. A consequence of the elongation of the droplet is that smaller droplets will be formed upon breaking by turbulence.

Independent of the mechanism of rupture, the newly formed droplets will present a part of their surface area not well covered by the surfactant, namely the surface of the droplets will be unevenly covered until surfactant diffusion brings the system to the equilibrium of adsorption.[18] During this period (and in some cases after establishing the equilibrium of adsorption), the droplets may coagulate.

Droplet break-up under elongational flow

Droplets will break up when the disruptive energy equals the surface energy and the viscoelastic energy.

$$\text{Disruptive energy} = \text{Surface energy} + \text{viscoelastic energy} \tag{1}$$

The disruptive energy is

$$\text{Disruptive energy} = \frac{\pi}{6} d_0^3 \tau_c \tag{2}$$

where d_0 is the diameter of the droplet and τ_c is the extensional energy per unit volume given by

$$\tau_c = \eta_c \dot{\gamma} \tag{3}$$

where η_c is the viscosity of the continuous phase and $\dot{\gamma}$ the shear rate. For 2D and 3D elongational flows the shear rate is[19]

$$2D : \dot{\gamma} = 2\dot{\varepsilon} \tag{4}$$

$$3D : \dot{\gamma} = \sqrt{3}\dot{\varepsilon} \tag{5}$$

where $\dot{\varepsilon}$ is the rate of elongation. Therefore, Eq. 3 can be written as

$$\tau_c = c_1 \eta_c \dot{\varepsilon} \tag{6}$$

The definition of the rate of elongation is of great importance. For the homogenizer valve depicted in Figure 6, $\dot{\varepsilon}$ was defined as[20]

$$\dot{\varepsilon} = \frac{u}{R_2} \tag{7}$$

where u is the velocity of the fluid through the gap and R_2 is a geometric characteristic of the homogenizer (Figure 6).

However, Phipps[21] defined $\dot{\varepsilon}$ as

$$\dot{\varepsilon} = \frac{u}{h} \tag{8}$$

where h is the slit width (Figure 6). This definition agrees better with that of Macosko[22] for an orifice

$$\dot{\varepsilon} = \frac{u}{a} \frac{\sin^3 \theta}{1 - \cos \theta} \tag{9}$$

where a is the radius of the orifice and θ the half angle of convergence of the flow approaching the orifice.

The velocity of the liquid is maximum at the entrance of the gap. At this point, it may be calculated as

$$u = \frac{Q}{2\pi R_o h} \tag{10}$$

where R_o is a geometric characteristic of the homogenizer (Figure 6).

Therefore, the disruptive energy is

$$\text{Disruptive energy} = c_2 d_0^3 \frac{\eta_c}{h^\alpha} \tag{11}$$

where $\alpha = 1$ or 2, depending on the definition of $\dot{\varepsilon}$ (Eqs. 7 and 8).

The surface energy is

$$\text{Surface energy} = \pi d_0^2 \sigma \tag{12}$$

where σ is the interfacial tension.

If the elastic component of the dispersed phase may be neglected, the viscous energy is

$$\text{Viscous energy} = \frac{\pi}{6} d_0^3 \tau_d \tag{13}$$

where τ_d is the viscous energy per unit volume (viscous stress within the drop). τ_d may be estimated as[23]:

$$\tau_d = \eta_d \, \dot{\gamma}_d = \eta_d \frac{u_d}{d_0/2} \tag{14}$$

where η_d is the viscosity of the dispersed phase, u_d the friction velocity within the droplet, and it was assumed that the velocity in the center of the droplet was zero. Hinze[23] proposed that u_d was proportional to $\sqrt{\tau_c/\rho_d}$, therefore

$$\text{Viscous energy} = c_3 d_0^3 \frac{\eta_d}{d_0} \sqrt{\frac{\eta_c}{\rho_d h^\alpha}} \tag{15}$$

Combination of Eqs. 11, 12, and 15 yields

$$c_2 d_0^3 \frac{\eta_c}{h^\alpha} = \pi d_0^2 \sigma + c_3 d_0^2 \eta_d \sqrt{\frac{\eta_c}{\rho_d h^\alpha}} \tag{16}$$

Therefore,

$$d_0 = c_4 \frac{h^\alpha}{\eta_c} \sigma + c_5 \frac{\eta_d}{\sqrt{\eta_c}} \frac{h^{\alpha/2}}{\rho_d^{1/2}} \tag{17}$$

It is worth pointing out that the viscosities that should be used in Eq. 17 are elongational viscosities. For Newtonian fluids, the elongational viscosity is about three times the shear viscosity (Trouton ratio). However, for non-Newtonian fluids this ratio is much higher. Therefore, for η_d the elongational viscosity was measured.

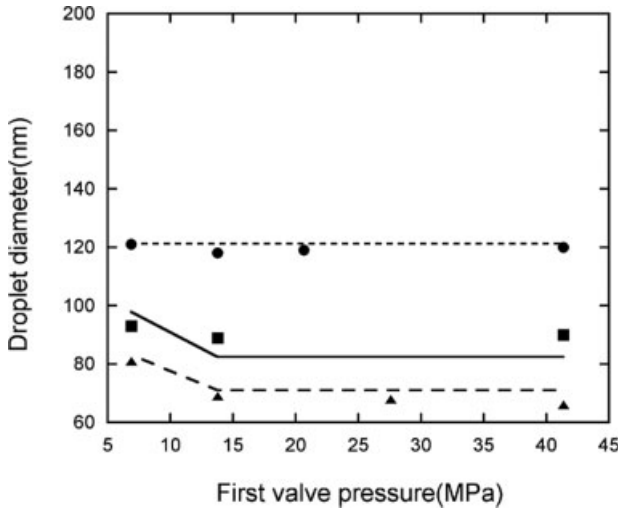

Figure 7. Fitting of the experimental data by the model for 15 wt % of resin and different emulsifier concentrations: 2 wt % (● experimental, - - - model); 4 wt % (■ experimental, —— model): 6 wt % (▲ Experimental, – – – model).

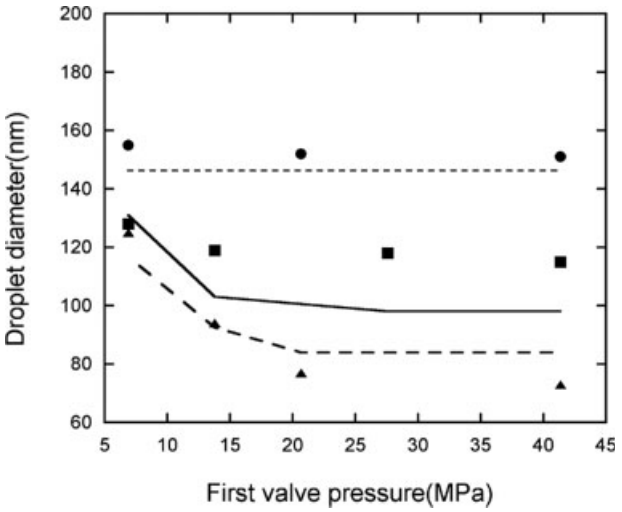

Figure 8. Fitting of the experimental data by the model for 30 wt % of resin and different emulsifier concentrations: 2 wt % (● experimental, - - - model); 4 wt % (■ experimental, —— model): 6 wt % (▲ experimental, – – – model).

The gap width can be calculated from the equation of the pressure drop that for laminar flow is[24]

$$\Delta P = \frac{\rho_e}{4}\left(\frac{Q}{2\pi R_0 h}\right)^2 + 6\frac{\eta_e Q}{\pi h^3}\ln\frac{R_2}{R_0} + \frac{\rho_e}{2}\left(\frac{Q}{2\pi R_2 h}\right)^2 \quad (18)$$

where ρ_e and η_e are the density and viscosity of the emulsion. For turbulent flow, the second term of the right side of Eq. 18 should be replaced by[25]

$$5\frac{\rho_e \upsilon_e^{3/5}}{h^3}\left(\frac{Q}{2\pi}\right)^{7/5}\left(\frac{1}{R_0^{2/5}} - \frac{1}{R_2^{2/5}}\right) \quad (19)$$

where $\upsilon_e = \eta_e/\rho_e$.

The dimensions of the equipment used in this work are

$$R_0 = 0.00165 \text{ m}; \quad R_2 = 0.0024 \text{ m}; \quad Q = 60L/h \quad (20)$$

According to Phipps,[21] the transition from laminar to turbulent flow occurs at

$$Re = \frac{Q\rho_e}{2\pi R_0 \eta_e} = 500 \quad (21)$$

Equation 18 shows that

$$h = c_6\ \Delta P^{-\beta_1} \quad (22)$$

with $0.33 < \beta_1 < 0.5$.

In addition, for a fixed pressure drop,

$$h \propto \eta_e^{\beta_2} \text{ with } \beta_2 < \frac{1}{3} \quad (23)$$

Therefore, the maximum size of the droplet that can be broken up is

$$d_0 = c_7\frac{\eta_e^{\alpha_1}}{\Delta P^{\alpha_2}} + c_8\frac{\eta_d \eta_e^{0.5\alpha_1}}{\Delta P^{0.5\alpha_2}} \quad (24)$$

where the viscosity, the interfacial tension, and the density of the continuous phase, as well as the density of the dispersed phase were integrated in the coefficients. The units of the variables are η_e (mPa s); η_d (mPa s), ΔP (MPa), and d_0 (nm).

Equation 24 predicts that the maximum droplet size that can be broken-up decreases with the pressure of the homogenizer

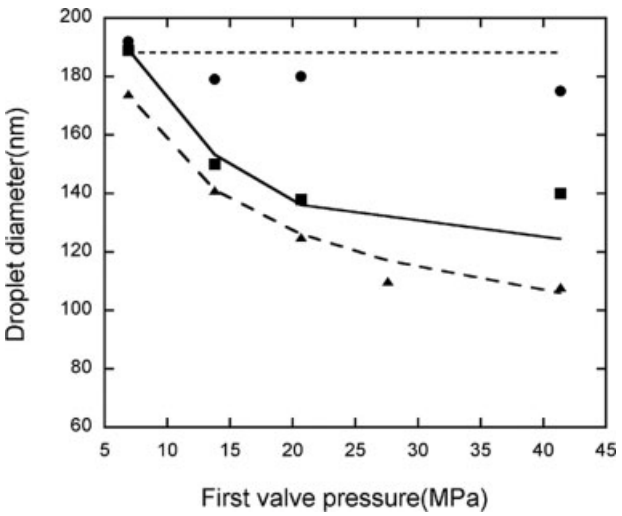

Figure 9. Fitting of the experimental data by the model for 50 wt % of resin and different emulsifier concentrations: 2 wt % (● experimental, - - - model); 4 wt % (■ experimental, —— model): 6 wt % (▲ experimental, – – – model).

Table 4. Values of the Parameters of the Model

	c_7	c_8	α_1	α_2	c_{11}	c_{12}	c_{13}	c_{15}
Varying Hamaker constant (Eq. 32)	134.66	1.14	0.084	0.43	1.42×10^{-5}	0.71	1.87	0.40
Single Hamaker constant	103.70	1.0	0.12	0.35	1×10^{-5}	1.33	0	0.48

and increases with the emulsion viscosity, the viscosity of the dispersed phase, and the interfacial tension.

Droplet coagulation

Miniemulsions may degrade by both diffusional degradation (Ostwald ripening) and by droplet coagulation. Diffusional degradation is strongly reduced by using costabilizers (low–molecular-weight highly water insoluble compounds[26,27]). In addition, the combination of costabilizers (SA in this work) with polymers (alkyd resin) is a very efficient way of minimizing Ostwald ripening.[28] Therefore, droplet coagulation was the only mechanism considered for droplet degradation.

The rate for droplet coagulation is

$$\frac{dN}{dt} = -kN^2(\text{droplet L}^{-1}\ \text{s}^{-1}) \tag{25}$$

where k is the coagulation rate coefficient and N is the number of droplets per unit volume of miniemulsion.

The coagulation rate coefficient is[29]

$$k = \frac{k_{\text{fast}}}{W} \tag{26}$$

where k_{fast} is the coagulation rate coefficient in the absence of an energy barrier

$$k_{\text{fast}} = \frac{8k_BT}{3\eta_c}(\text{L}\ \text{s}^{-1}) \tag{27}$$

and W is the Fuchs stability ratio

$$W = \frac{1}{2\kappa d}\exp(V_{T_{\max}}/k_BT) \tag{28}$$

where κ is the Debye–Hückel parameter, η_c the viscosity of the continuous phase, d the diameter of the droplet, $V_{T_{\max}}$ the maximum value of the total interaction potential, and k_B the Boltzmann constant. For a symmetric monovalent salt at 25°C in water, the Debye–Hückel parameter is[30]

$$\kappa = 3.288\sqrt{I}\ (\text{nm}^{-1}) \tag{29}$$

where I is the ionic strength (in mol/L).

The total potential of interaction at the distance b is

$$V_T = \pi\varepsilon d\left(\frac{4k_BT}{ze}\right)^2\gamma^2\ln(1+\exp(-\kappa b)) - \frac{Ad}{24b} \tag{30}$$

where ε is the permittivity of the medium, A the Hamaker constant and γ is

$$\gamma = \tanh\left(\frac{ze\psi_0}{4k_BT}\right) \tag{31}$$

with z being the valency of the counterion, e the electron charge, and ψ_0 the surface potential.

The effective Hamaker constant was assumed to be a linear function of the resin content.

$$A = c_9 + c_{10}\phi_R \tag{32}$$

where ϕ_R is the content of resin in the organic phase.

For the distance $b = b^*$ at which $V_T = V_{T_{\max}}$

$$V_{T_{\max}} = \pi\varepsilon d\left(\frac{4k_BT}{ze}\right)^2\tanh^2\left(\frac{ze\psi_0}{4k_BT}\right)\ln\left(1+\exp\left(-c_{11}\sqrt{I}\right)\right) - (c_{12}+c_{13}\phi_R)d \tag{33}$$

The Gouy–Chapman equation relates the surface potential with the surface charge density, σ_0

$$\sigma_0 = (8C_0N_A\varepsilon k_BT)^{0.5}\sinh\left(\frac{ze\psi_0}{2k_BT}\right) \tag{34}$$

where C_0 is the ionic concentration.

The surface charge density was assumed to be proportional to the surface concentration of emulsifier

$$\sigma_0 = \frac{c_{14}E_TN_A2e}{A_d} \tag{35}$$

where E_T is the total amount of emulsifier (which according to Figure 5 is approximately equal to the amount of emulsifier adsorbed on the droplets) and A_d the surface area of the droplets given by

$$A_d = \pi d^2N \tag{36}$$

For a volume fraction of the dispersed phase ϕ, the relationship between d and N is

$$d = \left(\frac{6\ \phi}{\pi N}\right)^{1/3}(1\times10^8)(\text{nm}) \tag{37}$$

Combinations of Eqs. 27–37 (using $k_B = 1.38 \times 10^{-23}\ \text{J K}^{-1}$, $e = 1.602 \times 10^{-19}$ C, $T = 298$ K, $\eta_c = 1 \times 10^{-3}$ Pa s, $z = 1$, and $\varepsilon = 6.95 \times 10^{-10}\ \text{C}^2\ \text{N}^{-1}\text{m}^{-2}$) yields the following set of equations describing the coagulation rate coefficient.

Table 5. Viscosities of the Organic Phase

Alkyd Resin Content (wt %)	Elongational Viscosity (mPa s)
15	14
30	50
50	112

Table 6. Miniemulsion Viscosities (mPa s)

First/Second Valve Pressures (MPa)	2% Dowfax	4% Dowfax	6% Dowfax
15 wt % alkyd resin			
6.9/0.69	22	74	9
13.8/1.38	22	75	10
20.7/2.07	22		
27.6/2.76			12
41.4/4.14	23	79	11
30 wt % alkyd resin			
6.9/0.69	30	80	15
13.8/1.38		84	17
20.7/2.07	30		18
27.6/2.76		92	
41.4/4.14	30	93	20
50 wt % alkyd resin			
6.9/0.69	33	98	24
13.8/1.38	35	104	26
20.7/2.07	37	111	30
27.6/2.76			37
41.4/4.14	41	132	35

$$k = \frac{k_{\text{fast}}\left(6.576\sqrt{I}d\right)}{\exp\left(5.61d\tanh^2(9.73\psi_0)\ln\left(1+\exp(-c_{11}\sqrt{I})\right)-(c_{12}c_{13}\phi_{\text{R}})d\right)} \tag{38}$$

$$\sinh(19.47\psi_0) = c_{15}\frac{E_{\text{T}}d}{\sqrt{C_0}} \tag{39}$$

where c_{11}, c_{12}, c_{13}, and c_{15} are parameters of the model and $k_{\text{fast}} = 1.097 \times 10^{-14}$ L s^{-1}. The units of the variables are I, C_0, and E_{T} (mol L^{-1}); d (nm); and ψ_0 (V).

The initial condition for Eq. 25 is that the initial number of droplets is that formed by droplet break-up, which has a size d_0 (Eq. 24), and therefore

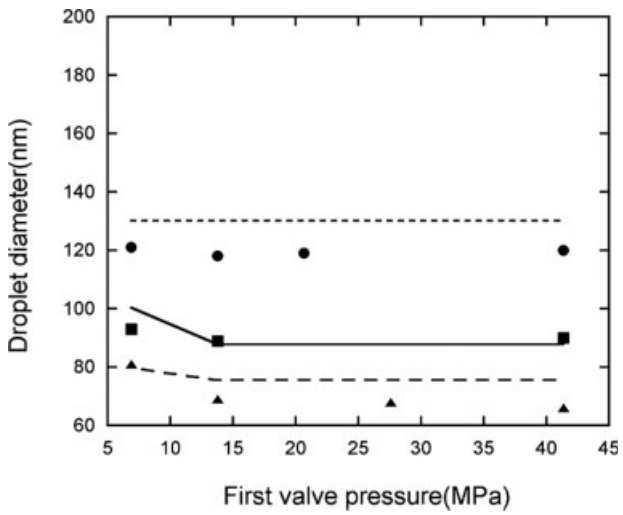

Figure 10. Fitting of the experimental data by the model (single Hamaker constant) for 15 wt % of resin and different emulsifier concentrations: 2 wt % (● experimental, - - - model); 4 wt % (■ experimental, —— model): 6 wt % (▲ experimental, – – – model).

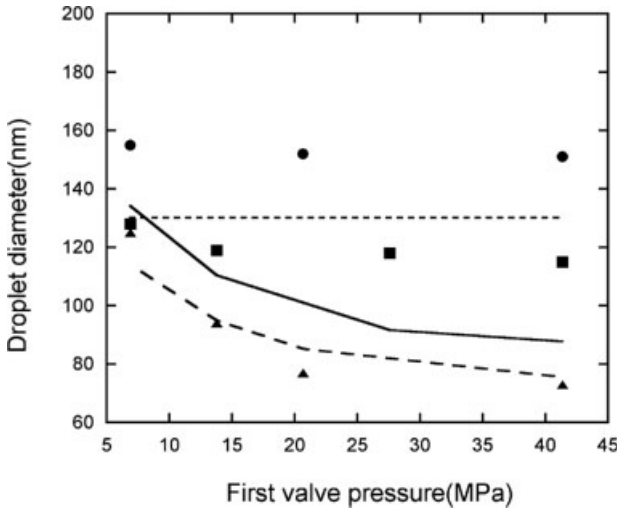

Figure 11. Fitting of the experimental data by the model (single Hamaker constant) for 30 wt % of resin and different emulsifier concentrations: 2 wt % (● experimental, - - - model); 4 wt % (■ experimental, —— model): 6 wt % (▲ experimental, – – – model).

$$\text{At } t = 0, \quad N_0 = \frac{6\times10^{24}\phi}{\pi d_0^3}(\text{droplet L}^{-1}) \tag{40}$$

The parameters of the model were estimated by fitting the experimental data in Figures 2–4. A Nelder–Mead algorithm of direct search was used. Figures 7–9 present the fitting of the data by the model with the values of the parameters in Table 4 and the experimental values of the viscosities (Tables 5 and 6). It can be seen that the model was able to

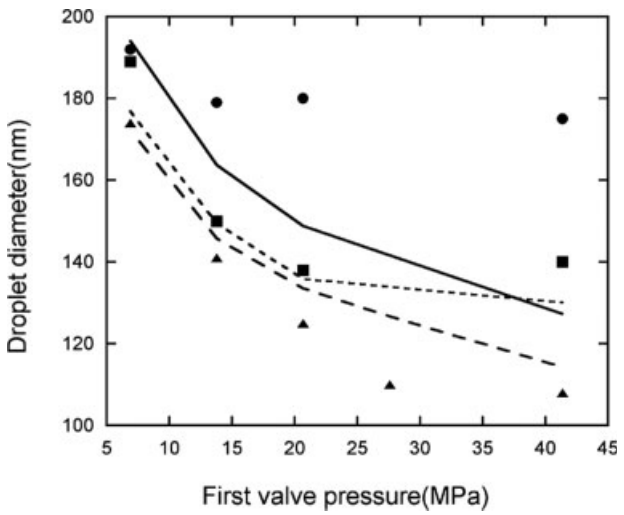

Figure 12. Fitting of the experimental data by the model (single Hamaker constant) for 50 wt % of resin and different emulsifier concentrations: 2 wt % (● experimental, - - - model); 4 wt % (■ experimental, —— model): 6 wt % (▲ experimental, – – – model).

predict quite precisely the experimentally observed trends. According to the model, both the viscosity of the organic phase (which affects droplet break-up) and the Hamaker constant (which affects coagulation rate) determined the effect of the resin content on the droplet size.

In order to illustrate the effect of the resin content on coagulation kinetics, the experimental data were fitted with a model in which a single Hamaker constant was used for all experiments. The values of parameters for this case are included in Table 4. Figures 10–12 show the fitting of this model. Comparison with Figures 7–9 show that a worse fitting was obtained, as the model using a single Hamaker constant could not catch the effect of the resin content.

Conclusions

The mechanism of formation of hybrid polymer–monomer waterborne miniemulsions in a high-pressure homogenizer was investigated. It was found that droplet size was the result of two consecutive processes: droplet break-up and coagulation. The final droplet size was determined by the mechanism giving the largest droplet size. Droplet break-up was a size-controlling mechanism at low pressures of the valve and high emulsifier concentrations, when the amount of emulsifier was enough to stabilize the droplets. Droplet coagulation determined the size of the droplets at high pressures and relatively low emulsifier concentrations, which were not enough to stabilize the large surface area created.

A mathematical model which accounted for both droplet break-up and coagulation was developed. It was considered that droplet break occurred when the disruptive energy equalled the surface energy and the viscoelastic energy. In the model, the resin content affected both the droplet break-up (through the viscosity of the organic phase) and the coagulation kinetics (through the Hamaker constant, which increased with the resin content). The model fitted well the experimental observations.

Acknowledgments

The financial support from the European Union (NAPOLEON NMP3-CT-2005-011844), the Diputación Foral de Gipuzkoa, and the Ministerio de Ciencia y Tecnología (CTQ2006-03412) projects is gratefully acknowledged.

Literature Cited

1. Shinnar R, Church JM. Predicting particle size in agitated dispersions. *J Ind Eng Chem*. 1960;52:253–256.
2. Chatzi EG, Kiparissides C. Steady-state drop-size distributions in high holdup fraction dispersion systems. *AIChE J*. 1995;41:1640–1652.
3. Calabrese RV, Changm TPK, Dang PT. Drop breakup in turbulent stirred-tank contactors. I. Effect of dispersed-phase viscosity. *AIChE J*. 1986;32:657–666.
4. Schultz S, Wagner G, Urban K, Ulrich J. High-pressure homogenization as a process for emulsion formation. *Chem Eng Technol*. 2004;27:361–368.
5. Antonietti M, Landfester K. Polyreactions in miniemulsions. *Prog Polym Sci*. 2002;27:689–757.
6. Asua JM. Miniemulsion polymerization. *Prog Polym Sci*. 2002; 27:1283–1346.
7. El-Aasser MS, Sudol ED. Miniemulsions: overview of research and applications. *JCT Res*. 2004;1:20–31.
8. Schork JF, Luo Y, Smulders W, Russum JP, Butté A, Fontenot K. Miniemulsion polymerization. *Adv Polym Sci*. 2005;175:129–255.
9. Rodríguez R. *Silicone-Modified Acrylic Nanoparticles by Miniemulsion Polymerization*, PhD Dissertation. University of the Basque Country, Spain 2007.
10. Arevalillo A, Do Amaral M, Asua JM. Rheology of concentrated polymeric dispersions. *Ind Eng Chem Res*. 2006;45:3280–3286.
11. Okubo M, Yamada A, Matsumoto T. Estimation of morphology of composite polymer emulsion particles by the soap titration method. *J Polym Sci Polym Chem Ed*. 1980;18:3219–3228.
12. Piirma I, Chang M. Emulsion polymerization of styrene: nucleation studies with nonionic emulsifier. *J Polym Sci Polym Chem Ed*. 1982;20:489–498.
13. Ozdeger E, Sudol ED, El-Aasser MS, Klein A. Role of the nonionic surfactant triton X-405 in emulsion polymerization. I. Homopolymerization of styrene. *J Polym Sci Part A: Polym Chem*. 1997;35: 3813–3825.
14. Floury J, Bellettre J, Legrand J, Desrumaux A. Analysis of a new type of high pressure homogenizer. A study of the flow pattern. *Chem Eng Sci*. 2004;59:843–853.
15. Grace HP. Dispersion phenomena in high viscosity immiscible fluid systems and application of static mixers as dispersion devices in such systems. *Chem Eng Commun*. 1982;14:225–277.
16. Floury J, Legrand J, Desrumaux A. Analysis of a new type of high pressure homogenizer. Part B. Study of droplet break-up and recoalescence phenomena. *Chem Eng Sci*. 2004;59:1285–1294.
17. Merrill EW, Leopairat P. Scission of noninterpenetrating macromolecules in transient extensional flows. *Polym Eng Sci*. 1980;20:505–511.
18. Brosel S, Schubert H. Investigations on the role of surfactants in mechanical emulsification using a high-pressure homogenizer with an orifice valve. *Chem Eng Process*. 1999;38:533–540.
19. Janssen JMH, Meijer HEH. Droplet breakup mechanisms: stepwise equilibrium versus transient dispersion. *J Rheol*. 1993;37:597–608.
20. Shamlou PA, Siddiqi SF, Titchener-Hooker NJ. A physical model of high-pressure disruption of Baker's yeast cells. *Chem Eng Sci*. 1995;50:1383–1391.
21. Phipps LW. The fragmentation of oil drops in emulsions by a high-pressure homogenizer. *J Phys D: Appl Phys*. 1975;8:448–462.
22. Macosko CW. *Rheology, Principles, Measurements and Applications*. New York: VCH Publishers, 1994:326–332.
23. Hinze JO. Fundamentals of the hydrodynamic mechanism of splitting in dispersion processes. *AIChE J*. 1955;1:289–295.
24. Nakayama Y. Action of the fluid in the air-micrometer (3rd report, characteristics of doublé-disc nozle No. 1, in the case of compressibility being ignored). *Bull JSME*. 1964;7:698–707.
25. Kawaguchi T. Entrance loss for turbulent flow without swirl between parallel discs. *Bull JSME*. 1971;14:355–363.
26. Higuchi WI, Misra J. Physical degradation of emulsions via the molecular diffusion route and its possible prevention. *J Pharm Sci*. 1962;51:459–466.
27. Ugelstad J, Moerk PC, Kaggerud KH, Ellingsen T, Berge A. Swelling of oligomer–polymer particles. New methods of preparation of emulsions and polymer dispersions. *Adv Colloid Interface Sci*. 1980;13:101–140.
28. Miller CM, Blythe PJ, Sudol ED, Silebi CA, El-Aasser MS. Effect of the presence of polymer in miniemulsion droplets on the kinetics of polymerization. *J Polym Sci Part A: Polym Chem*. 1994;32:2365–2376.
29. Fitch RM. *Polymer Colloids. A Comprehensive Introduction*. San Diego: Academic Press, 1997.
30. Hunter R J. *Foundations of Colloid Science, Vol 1*. New York: Oxford University Press, 1987:332–333.

Manuscript received July 19, 2007, and revision received Oct. 3, 2007.